

Use of the Boron partition coefficient ' K_D ' and B/Ca from planktonic foraminifera in the estimation of past seawater pCO₂

SUSHANT S. NAIK^{*1} and P. DIVAKAR NAIDU¹

¹ CSIR-National Institute of Oceanography, Dona-Paula, Goa, 403004, INDIA

*For correspondence, email:sushant@nio.org

Tel: +91 832 2450657; Fax: +91 832 2450602

Abstract

We assess the usefulness of the empirical boron partition coefficient, K_D and B/Ca measured from planktonic foraminifera in estimation of pCO₂ using three different relationships between K_D and temperature derived from various studies. Two sediment cores spanning the last 22 kyr were utilised, one from the intense CO₂ source region of the Western Arabian Sea (WAS) and another from the Eastern Arabian Sea (EAS). The sea-air difference in pCO₂ at these sites shows results contrary to the present day scenario. Moreover the reconstructions using the three K_D relationships lead to assorted results which suggests that the K_D approach may not be suitable in paleo-pCO₂ reconstructions.

Keywords: boron, foraminifera, Arabian Sea, pCO₂, partition coefficient

INTRODUCTION

Boron exists in seawater as borate (B(OH)₄⁻) or boric acid (B(OH)₃) depending upon seawater pH, with a greater abundance of B(OH)₃ at lower pH and B(OH)₄⁻ at higher pH. Since dissolved B(OH)₄⁻ is considered to be the species incorporated into foraminiferal calcite, B/Ca should increase with greater abundance of borate. Boron incorporation in foraminifera shells will thus be greater if the seawater is more alkaline. Therefore, foraminiferal B/Ca, is thought to be a potential proxy for pH and pCO₂ (Yu *et al.*, 2007; Tripathi *et al.*, 2009). Yu *et al.*, 2007, used B/Ca ratios and the empirical boron partition coefficient, K_D ($= [B/Ca_{CaCO_3}] / [B(OH)_4^-]/[HCO_3^-]_{seawater}$) to estimate seawater borate/bicarbonate ratios ($[B(OH)_4^-]/[HCO_3^-]$) and reproduce two glacial–interglacial cycles of pCO₂. In the modern seawater, $[B(OH)_4^-]/[HCO_3^-]_{seawater}$ is proportional to pH as the concentration of B(OH)₄⁻ increases and HCO₃⁻ decreases with increasing seawater pH. If we measure B/Ca from foraminifera and K_D is estimated from temperature (core-top K_D variability is attributed to the influence of temperature on boron partitioning) (Yu *et al.*, 2007), we can calculate $[B(OH)_4^-]/[HCO_3^-]$

$[\text{B}]_{\text{seawater}}$ and hence pH and pCO_2 . Tripathi *et al.*, 2009 have used B/Ca ratios in the planktonic foraminifera, *Globigerinoides ruber* and *Globigerinoides sacculifer* from the western tropical Pacific to reveal that during the Middle Miocene, atmospheric pCO_2 may have been similar to modern levels. However, a recent study from the upwelling region of the Arabian Sea shows that B/Ca is not related to salinity, pH or DIC but boron incorporation in planktonic foraminifera maybe size-related (Naik and Naidu, 2014). It was also observed that the calibrations using K_D can sometimes be driven by the relationship between $[\text{B}(\text{OH})_4^-]/[\text{HCO}_3^-]$ and seawater parameters and not by B/Ca (Allen and Hönisch, 2012). In this study we test the effectiveness of K_D in estimation of pCO_2 using different K_D relationships, applied to two sediment cores from the Arabian Sea.

SAMPLES AND METHODS

The Western Arabian Sea core (ODP Site 723A; 18°03'N and 57°37'E; wd = 808 m) and the Eastern Arabian Sea core (AAS9/21; 14°30'N and 72°39'E; wd = 1807 m) are from above lysocline depths (Fig. 1). Both these cores cover the last ~22kyr period. The details of the Age Model, B/Ca, Mg/Ca and $\delta^{18}\text{O}$ measurements and data are described in Naik and Naidu, 2014. CO_2 system calculations were performed using a Microsoft Excel-based programme ($\text{CO}_2\text{sys_v2.1}$) (Lewis and Wallace, 1998). The input parameters for this programme were salinity, temperature, alkalinity, total CO_2 and nutrients, and the constants used were as follows : pK^*B and KHSO_4 are from Dickson, 1990, the relationship between total B in seawater and chlorinity from Lee *et al.*, 2010 and K_1 & K_2 carbonate disassociation constants from Lueker *et al.*, 2000. pH calculations were done on the 'total scale'. pCO_2 calculations were done using different K_D equations; 1. constant K_D ($K_D = 0.0015$) (Yu *et al.*, 2007); 2. temperature sensitive K_D for *G.ruber* from Yu *et al.*, 2007 ($K_D = 0.047 * \text{EXP}(0.131 * \text{Mg/Ca-SST})$); and 3. temperature sensitive K_D for *G.ruber* from Tripathi *et al.*, 2009 ($K_D = 0.211 * \text{EXP}(0.064 * \text{Mg/Ca-SST})$).

RESULTS AND DISCUSSION

The Arabian Sea is influenced by the south-west (SW) monsoon winds during the northern hemisphere summer and north-east (NE) monsoon winds during winter (Wyrтки 2009). The strong south-westerly monsoon winds cause offshore Ekman transport and intense seasonal upwelling along the Oman and Somalia margins and weak upwelling along some parts of the east coast of India (Wyrтки 2009). The upwelled waters are laden with high CO_2 and the western Arabian Sea (WAS) in comparison to the eastern Arabian Sea (EAS) is thus an intense CO_2 source to the atmosphere with pCO_2 values reaching ~600 μatm during the SW monsoon (Sarma, 2003).

B/Ca ratios at ODP Site 723A ranged from 124 to 179 $\mu\text{mol/mol}$ and in Core AAS9/21 they ranged from 117 to 132 $\mu\text{mol/mol}$ for the last 22 kyr (Naik and Naidu, 2014). By using B/Ca data, reconstructed salinity and temperature from the cores ODP723A and AAS9/21 and different K_D relationships, we calculated borate/bicarbonate ratios and subsequently the pCO_2 . At ODP Site 723A, reconstructed pCO_2 varies from 110 to 286 ppmv which is atypical of this region wherein present day pCO_2 values reach up to 700 ppmv during the South-West Monsoon and is a strong source of CO_2 to the atmosphere (Sarma, 2003). As seen at ODP Site 723A, though the pCO_2 pattern using the three K_D relationships is the same, the differences in pCO_2 reconstructed using these equations is large, of up to 100 ppmv (Fig. 2). Lowest pCO_2 values are noticed between 9 to 12 kyr. However on the contrary, pCO_2 reconstruction using the more reliable boron isotopes in this region show highest pCO_2 values at 12 kyr corresponding to the Younger Dryas period, due to an increase in the Asian Summer Monsoon (ASM) (Palmer *et al.*, 2010).

The core AAS9/21 shows an overall pCO_2 increase through the time period using the three K_D relationships, with pCO_2 values ranging from 158 to 429 ppmv. In comparison to modern day values (~ 400 ppmv; Sarma, 2003), the core-top pCO_2 reconstruction using the K_D relationship by Yu *et al.*, 2007 (Fig. 2) gives a rather closer comparison. The pCO_2 pattern using the three relationships are similar but the difference between the reconstructions is very large of up to 178 ppmv at 2.55 kyr. Moreover the EAS is a weaker upwelling region in comparison to the WAS, but the pCO_2 reconstructions give a different picture showing higher pCO_2 in the EAS and lower in the WAS. This can be better illustrated based on the ΔpCO_2 , which is calculated as the difference in pCO_2 obtained from the sediment cores (pCO_2^{sw}) and the ice-core CO_2 ($\text{pCO}_2^{\text{atm}}$) record (Smith *et al.*, 1999) over time, $\Delta\text{pCO}_2 = \text{pCO}_2^{\text{sw}} - \text{pCO}_2^{\text{atm}}$ (Fig. 3). Using the three K_D relationships, it was seen that ODP Site 723A was a sink of atmospheric CO_2 throughout the study period, with ΔpCO_2 ranging from 12 to -152 ppmv. However as seen earlier, this site is well-known to be a strong source of CO_2 to the atmosphere. Results from the EAS are as well contrary to the modern day scenario. ΔpCO_2 at AAS9/21 ranged from 167 to -81 ppmv. ΔpCO_2 calculated using the two K_D approaches, constant K_D and temperature sensitive K_D by Yu *et al.*, 2007, show that Site AAS9/21 was a source of atmospheric CO_2 for the last 22 kyr whereas the third K_D relationship by Tripathi *et al.*, 2009, depict this site as a CO_2 sink. Thus, the reconstructed pCO_2 using different K_D approach give an assorted picture and are contradictory to what is known about western and the eastern Arabian Sea, in the modern times.

CONCLUSIONS

The present study illustrates the problems of the ' K_D ' approach. The $p\text{CO}_2$ calculated using the three K_D equations provide variable results with differences in $p\text{CO}_2$ values which are much larger compared to a glacial-interglacial CO_2 shift. The inconsistencies observed in estimation of $p\text{CO}_2$ thus indicate that the use of K_D should be avoided until we gain significant knowledge on relative impacts of different chemical species on boron incorporation.

Acknowledgements:

SSN is grateful to INDO-US Science and Technology Forum for providing the fellowship to work at the LDEO. A set of samples was provided by the Ocean Drilling Program, which is sponsored by the U.S. National Science Foundation and participating countries under the management of the Joint Oceanographic Institutions. This is National Institute of Oceanography contribution No.

REFERENCES:

1. Allen, K. A. and Hönisch, B. (2012) The planktic foraminiferal B/Ca proxy for seawater carbonate chemistry: A critical evaluation. *Earth Planet. Sci. Lett.* **345-348**, 203–211. doi:10.1016/j.epsl.2012.06.012.
2. Dickson, A. G. (1990) Thermodynamics of the dissociation of boric acid in synthetic seawater from 273.15 to 318.15 K. *Deep-Sea Res.* **37**, 755–766.
3. Lee, K., Kim, T.-W., Byrne, R. H., Millero, F. J., Feely, R. A. and Liu, Y.-M. (2010) The universal ratio of boron to chlorinity for the North Pacific and North Atlantic oceans. *Geochim. et Cosmochim. Acta.* **74**, 1801–1811. doi: 10.1016/j.gca.2009.12.027.
4. Lewis, E. and Wallace, D. W. R. (1998) CO2SYS—Program developed for the CO_2 system calculations. *Carbon Dioxide Inf. Anal. Center; Report ORNL/CDIAC-105*.
5. Lueker, T. J., Dickson, A. G. and Keeling, C. D. (2000) Ocean $p\text{CO}_2$ calculated from dissolved inorganic carbon, alkalinity, and equations for K_1 and K_2 : validation based on laboratory measurements of CO_2 in gas and seawater at equilibrium. *Mar. Chem.* **70**, 105–119.
6. Naik, S. S. and Naidu, P. D. (2014) Boron/calcium ratios in *Globigerinoides ruber* from the Arabian Sea: Implications for controls on boron incorporation. *Mar. Micropal.* **107**, 1-7. doi: 10.1016/j.marmicro.2014.01.004.

7. Palmer, M. R., Brummer, G. J., Cooper, M. J., Elderfield, H., Greaves, M. J., Reichart, G. J., Schouten, S., and Yu, J. M. (2010) Multi-proxy reconstruction of surface water pCO₂ in the northern Arabian Sea since 29 ka. *Earth Planet. Sci. Lett.* **295**, 49–57. doi:10.1016/j.epsl.2010.03.023.
8. Sarma, V. V. S. S. (2003) Monthly variability in surface pCO₂ and net air-sea CO₂ flux in the Arabian Sea. *J. of Geophys. Res.* **108**(C8). 3255. doi:10.1029/2001JC001062.
9. Smith, H. J., Fischer, H., Wahlen, M., Mastroianni, D., and Deck, B. (1999) Dual modes of the carbon cycle since the Last Glacial Maximum. *Nature.* **400**, 248-250.
10. Tripathi, A. K., Roberts, C. D. and Eagle, R. A. (2009) Coupling of CO₂ and ice sheet stability over major climatic transitions of the last 20 million years. *Science.* **326**, 1394-1397. doi: 10.1126/science.1178296.
11. Wyrтки, K. (1973) Physical oceanography of the Indian Ocean. In: *Zeitzschelp, B. (Eds.) The Biology of the Indian Ocean. Springer- Verlag. New York.* pp.18–36.
12. Yu, J., Elderfield, H. and Hönisch, B. (2007) B/Ca in planktonic foraminifera as a proxy for surface seawater pH. *Paleoceanogr.* **22**, PA2202. doi:10.1029/2006PA001347.

Figure legends:

Fig. 1: Chlorophyll-*a* concentration from SeaWiFS (in mg/m³) during the south-west monsoon period; June–September, 1998 (source: <http://gdata1.sci.gsfc.nasa.gov/>) with overlaid core locations. The Western Arabian Sea is seen to be more productive than the eastern counterpart.

Fig. 2: The top panel shows pCO₂ reconstructed from ODP723A using constant K_D (squares, $K_D = 0.0015$); using temperature sensitive K_D for *G.ruber* from Yu et al. (2007) (circles, $K_D = 0.047 * EXP(0.131 * Mg/Ca-SST)$); and temperature sensitive K_D for *G.ruber* from Tripathi et al. (2009) (triangles, $K_D = 0.211 * EXP(0.064 * Mg/Ca-SST)$). The lower panel is the same as upper panel but for AAS9/21.

Fig. 3: The top panel shows ΔCO_2 (difference in CO₂ between sea and air; atmospheric CO₂ data taken from ice-core, Smith et al., 1999) using different K_D relationships as shown in Fig. 1. The lower panel is the same as upper panel but for AAS9/21.

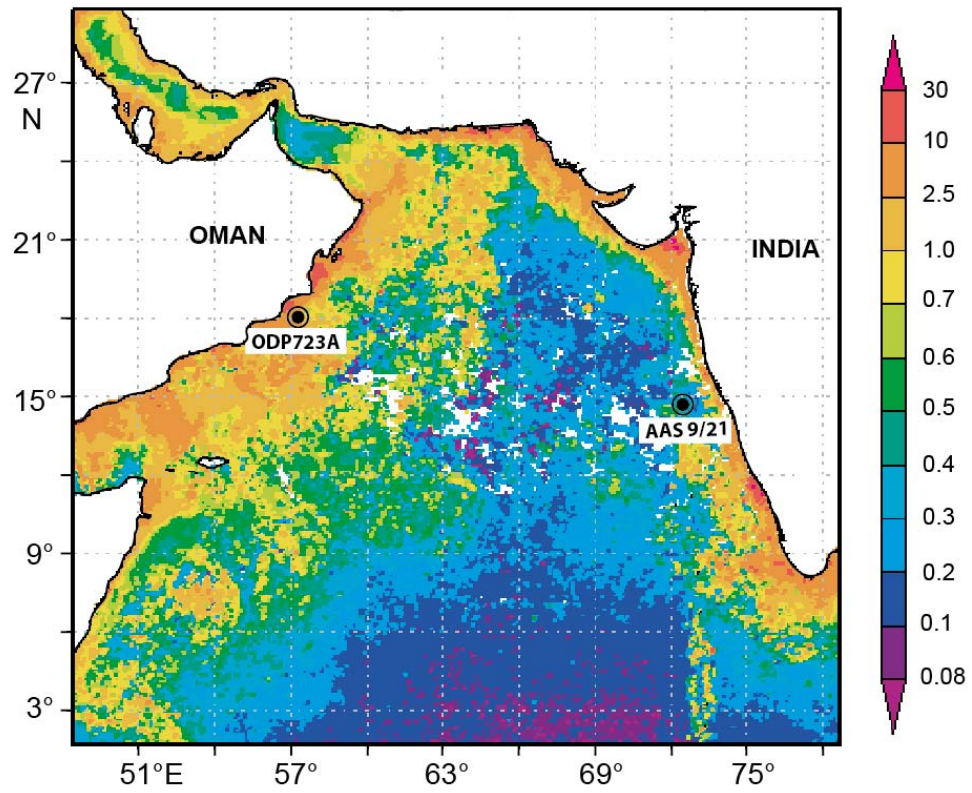


Fig. 1

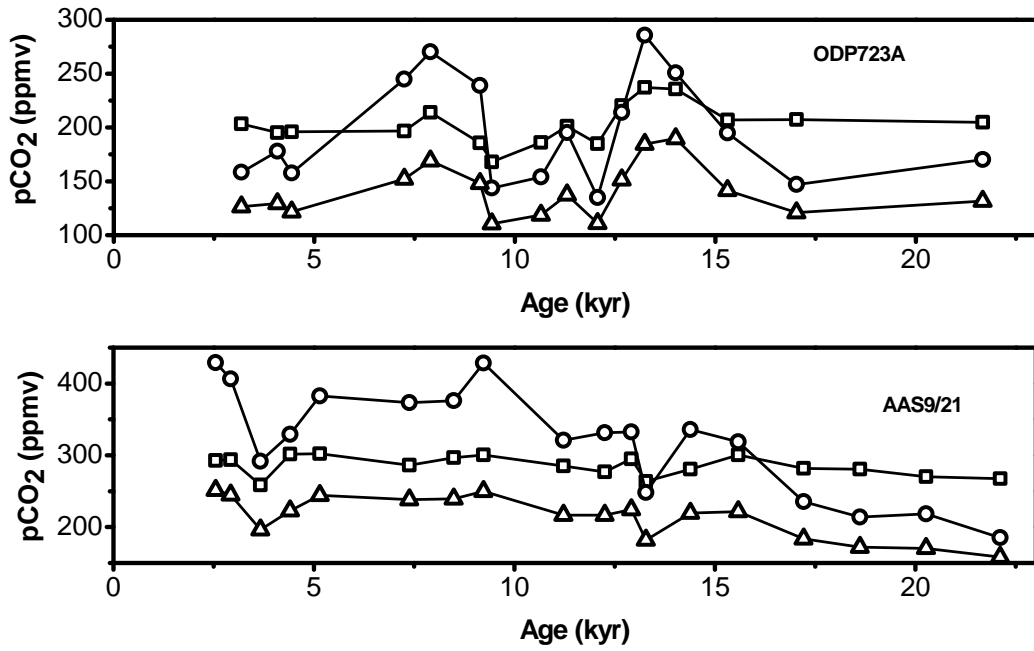


Fig. 2

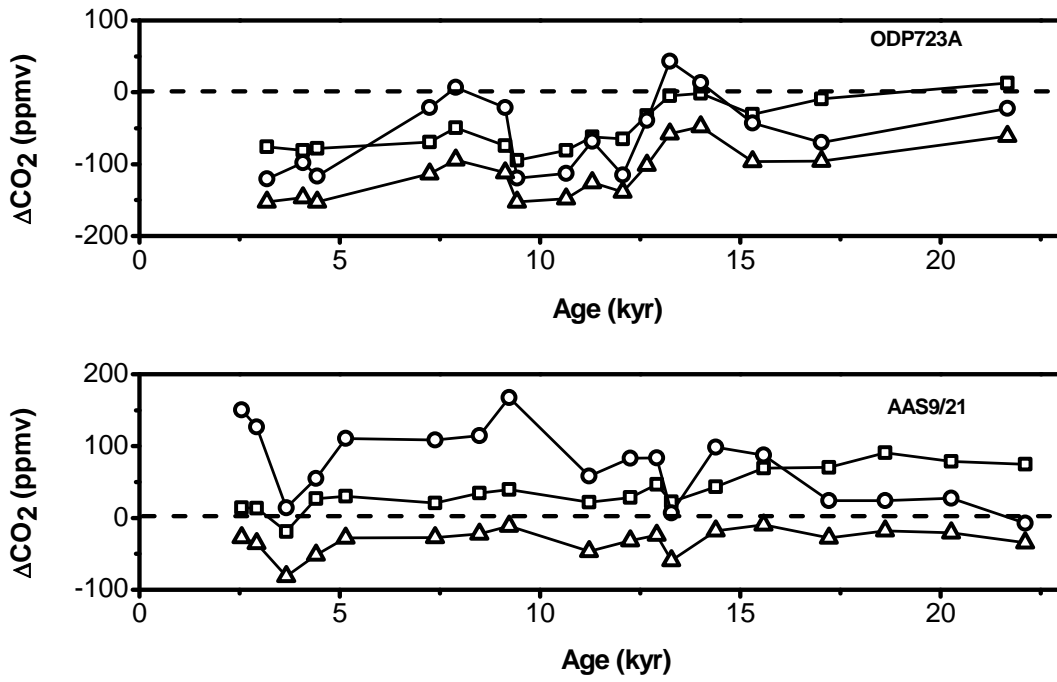


Fig. 3